

Single-pion production in $\bar{p}p$ interactions near threshold*

R. R. Burns, P. E. Condon, J. Donahue, M. A. Mandelkern,
L. Michelotti, L. R. Price, and J. Schultz
Department of Physics, University of California, Irvine, California 92664
(Received 25 November 1974)

Results are reported on the reaction $\bar{p}p \rightarrow \bar{N}N\pi$ at center-of-mass energies of 2.063, 2.094, and 2.114 GeV. The cross sections for π^0 production at these energies are 22 ± 7 , 35 ± 9 , and $126 \pm 26 \mu\text{b}$; those for π^- and π^+ production are 20 ± 7 , 41 ± 10 , and $79 \pm 20 \mu\text{b}$ and 16 ± 6 , 43 ± 10 , and $47 \pm 16 \mu\text{b}$, respectively. The cross section obeys the energy dependence of phase space and joins smoothly onto data at higher energies. The cross section as a function of energy is relatively well fitted by a calculation based on current-algebra predictions of soft-pion emission. Resonance production is small, but there is a possible $I=1$ enhancement which may be the $S(1930)$. Our highest energy $\bar{p}p \rightarrow \bar{p}p\pi^0$ channel may proceed approximately 50% through $\Delta(1236)\bar{p} + \bar{\Delta}(1236)p$. Predicted nonstrange exotic mesons coupled preferentially to $\bar{N}N$ and $\bar{N}N\pi$ are not seen.

I. INTRODUCTION

We have studied proton-antiproton collisions near threshold for the reactions

$$\bar{p}p \rightarrow \bar{p}p\pi^0, \quad (1)$$

$$\rightarrow \bar{p}n\pi^+, \quad (2)$$

$$\rightarrow \bar{n}p\pi^-. \quad (3)$$

These reactions have been studied at higher energies by a number of authors,¹ some of whom have compared their data to the predictions of the one-pion exchange model. Ma *et al.*² have carried out an isospin analysis of these and related processes. Since the energy region reported here is very near threshold, we discuss our experimental results in terms of a simple statistical model and the current-algebra predictions for soft-pion emission. Although the statistics reported on are not large, since the cross sections observed near threshold are one to two orders of magnitude lower than those previously reported, they allow for a significant comparison with these models.

II. EXPERIMENTAL PROCEDURE

The work presented here is based on 220 000 pictures taken in the BNL 30-in. hydrogen bubble chamber. Film was taken at six distinct beam momenta, with mean values 0.686, 0.772, 0.861, 0.943, 1.037, and 1.098 GeV/c at the chamber center. The 0.861-GeV/c data are above threshold for $\bar{p}p \rightarrow \bar{N}N\pi$; however, due to the smallness of the cross section there, only the data from the upper three momenta were used. We directly measured, without prescanning, all two-prong events. Approximately 20% of the film was remeasured to determine scanning and processing efficiencies.

The events were processed by the programs PANEL-TVGP-SQUAW.

We analyzed as inelastic scattering those events which did not have a 4C fit with $\chi^2 < 24$ to any two-body final state, and which had $\chi^2 < 2.7$ for one of the three channels (1)–(3). A proton or antiproton was usually identifiable by ionization. Several hundred poorly measured elastic scattering events fit the $\bar{p}n\pi^+$ hypothesis because of the fast forward antiproton in both cases. These events were easily identified since all had short stopping positive tracks which did not decay. We imposed, in addition, fiducial volume criteria and curvature and angle criteria for the beam track. The final numbers of events selected from the first pass are given in Table I. We believe the three channels to be well separated and contamination from other reactions to be less than 5%.

III. CROSS SECTIONS

The scanning-processing efficiency was found to be $(70 \pm 9)\%$. Since this is excellent agreement with the scanning-processing efficiency of $(68 \pm 2)\%$ found for other two-prong events in our film,³ we use the latter figure and its smaller error. The correction to the cross sections for the χ^2 cut was determined to be a factor of 1.1. A count of passing beam tracks in every tenth frame provided a flux measurement at each beam momentum. The cross sections are given in Table I and also shown in Figs. 1 and 2 along with higher-energy data.¹

Charge-conjugation invariance (or CP) requires the reactions (2) and (3) to have equal cross sections. The data are in good agreement with this requirement. Furthermore, in reaction (1) the center-of-mass angular distributions of the \bar{p}

TABLE I. The experimental results for the cross sections. The numbers of events are also given. Results are labeled by the pion in the final state of the $\bar{N}N \rightarrow \bar{N}N\pi$ reaction. The ratio R is defined by Eq. (4) in the text.

P_{beam} (GeV/c)	$E_{\text{c.m.}}$ (GeV)	Observed number of events			Cross sections (μb)			R
		π^0	π^-	π^+	$\sigma(\pi^0)$	$\sigma(\pi^-)$	$\sigma(\pi^+)$	
0.943	2.063	10	9	7	22 ± 7	20 ± 7	16 ± 6	1.2 ± 0.5
1.037	2.094	16	19	20	35 ± 9	41 ± 10	43 ± 10	0.8 ± 0.2
1.098	2.114	24	15	9	126 ± 26	79 ± 20	47 ± 16	2.0 ± 0.6

and the p should be reflections of each other, and the π^0 should be forward-backward symmetric. Similarly, the \bar{p} , n , and π^+ from reaction (2) should be reflections of the p , \bar{n} , and π^- , respectively, from reaction (3). The data are in good agreement with these predictions of charge-conjugation invariance. Therefore, the data from reactions (2) and (3) have been combined for the distributions presented below.

In Fig. 3 we show the variation with laboratory momentum of the ratio

$$R = \frac{\sigma(\pi^0)}{\frac{1}{2}[\sigma(\pi^+) + \sigma(\pi^-)]} \quad (4)$$

The final-state pion has been used to identify the appropriate channel.

IV. INVARIANT-MASS DISTRIBUTIONS

Figure 4 shows the invariant-mass distributions for the neutral and combined charged channels for

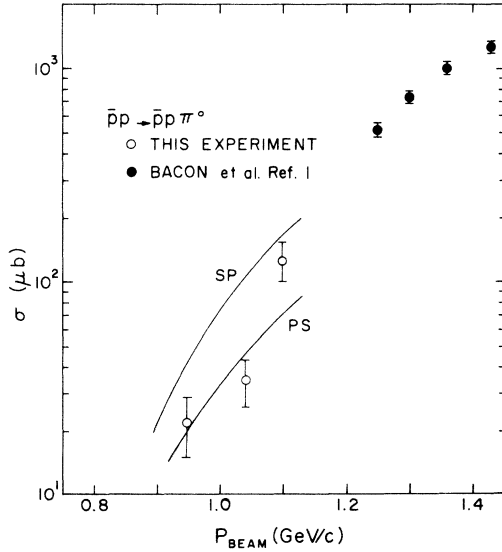


FIG. 1. Variation of the cross section for $\bar{p}p \rightarrow \bar{p}p\pi^0$ near threshold. The cross sections of Bacon *et al.* (Ref. 1) are also shown. The curves are the results of the phase-space (PS) and soft-pion (SP) models discussed in the text.

each energy and also the sums of the three energies. The curves drawn on this figure are phase spaces normalized to the number of events in each distribution.

The distributions are consistent with the phase-space predictions; however, they do show possible structure. In the nucleon-antinucleon mass plots, $M(\bar{p}p)$ with 55 events and $M(\bar{p}n, \bar{n}p)$ with 96 events, we estimate there are a few excess events above phase space in $M(\bar{p}p)$ just above $1.900 \text{ GeV}/c^2$, and about 15 events excess in $M(\bar{p}n, \bar{n}p)$ at $1.930 \text{ GeV}/c^2$. The dashed curve in the latter histogram is a phase-space fit to all bins except the one at $1.930 \text{ GeV}/c^2$, showing a marked excess of 15 events corresponding to about 2.5 standard deviations. This may be because of the controversial $S(1930)$ which has been reported in backward $\bar{p}p$ elastic scattering⁴ and more recently in the total $\bar{p}p$ and $\bar{p}d$ cross-section measurements of Carroll *et al.*⁵ Within our limited statistics, we conclude the enhancement is in $I=1$.

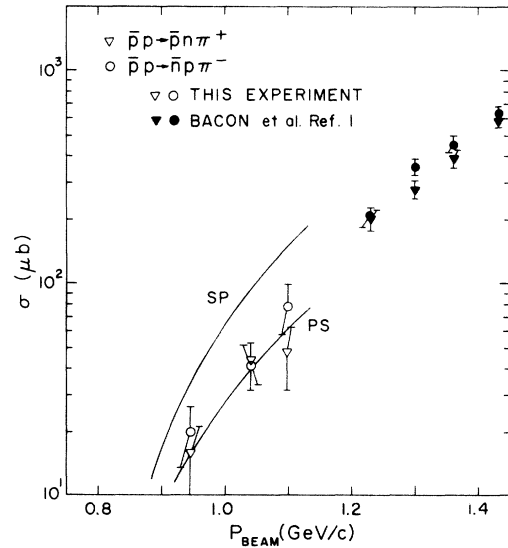


FIG. 2. Variation of the cross sections for $\bar{p}p \rightarrow \bar{p}n\pi^+$ and $\bar{p}p \rightarrow \bar{n}p\pi^-$ near threshold. The cross sections of Bacon *et al.* (Ref. 1) are also shown. The curves are the results of the phase-space (PS) and soft-pion (SP) models discussed in the text.

Our highest beam energy is only about a half-width below production threshold for the $\Delta(1236)$ [$\bar{\Delta}(1236)$] isobar. The accumulation of high-mass events in the $M(\bar{p}\pi^0, p\pi^0)$ distribution for the 2.114-GeV/ c^2 data may be due to some $\Delta(1236)$ and $\bar{\Delta}(1236)$ production. We estimate there to be about 12 events above phase space. The effect is not seen in the other $N\pi$ mass distributions.

V. DISCUSSION IN TERMS OF MODELS

The analysis by Ma *et al.*² in terms of an *incoherent* sum of isospin amplitudes corresponding to the diagrams of Figs. 5(a) and 5(b) showed that in the region from 1.1 to 1.5 GeV/ c the process is dominated by $I=1$, $I'=\frac{3}{2}$. This is perhaps to be expected since this is precisely the threshold region for producing $\Delta(1236)$ [and $\bar{\Delta}(1236)$]. In this analysis, pure $I'=\frac{3}{2}$ is characterized by a value of 2 for the ratio R . The statistical model gives $R=0.8$. Interference between the two diagrams may be important near threshold, and the ratio R may be sensitive not only to isospin channels, but to dynamical mechanisms as well.

Statistical Model. We first calculate the relative energy variation of the production cross section according to three-body phase space, which we would expect to dominate the energy dependence if production amplitudes vary little over the small

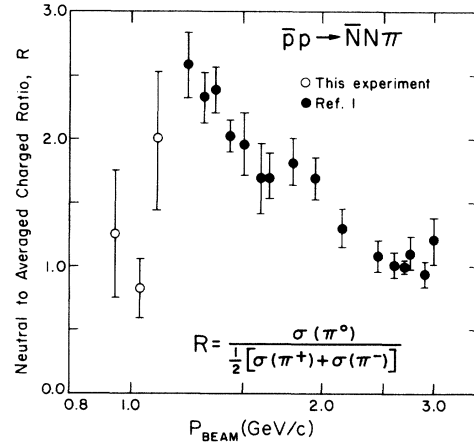


FIG. 3. Variation of the ratio R , the neutral-to-averaged-charged pion production cross sections, with beam momentum. Higher-energy data (Ref. 1) are also shown.

energy range studied. All three of the averaged charged-pion cross sections and the two lowest neutral-pion cross sections were used to fit the normalization and R . The best fit gave $R=1.0 \pm 0.2$. These results are shown on Figs. 1 and 2 labeled PS.

The difference between the experimental cross section for $\sigma(\pi^0)$ at the highest energy and this calculation is about $60 \mu\text{b}$. This corresponds to 12

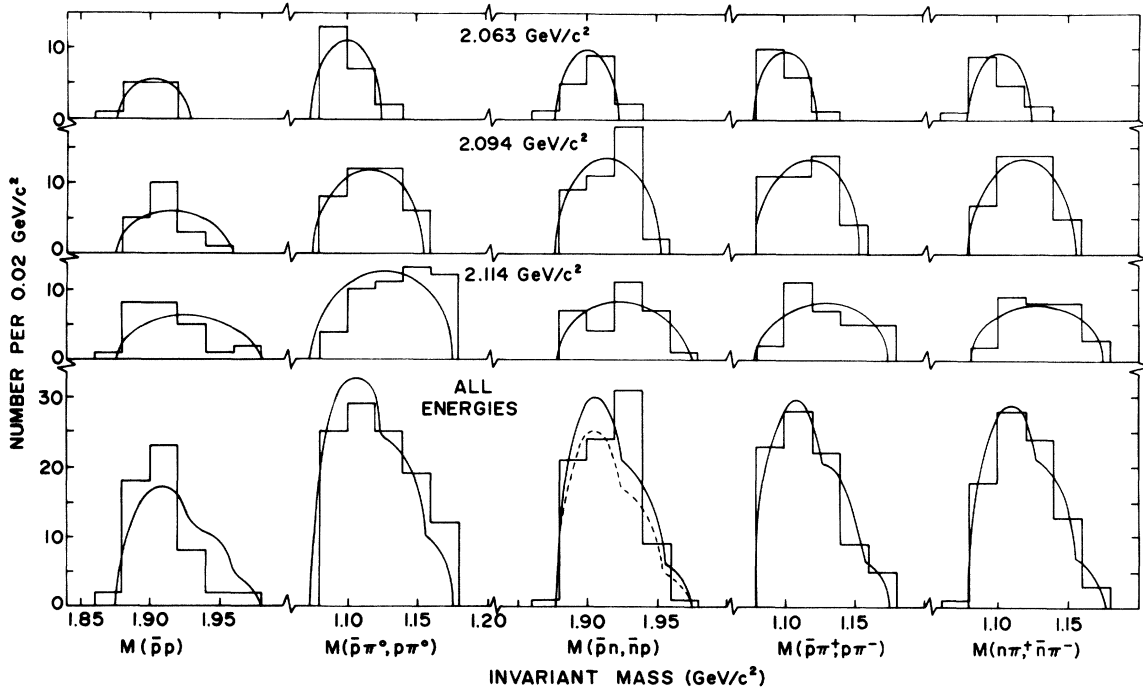


FIG. 4. Invariant-mass distributions. The charge-conjugate channels have been combined. The bottom set of distributions is all three energies combined. The curves are three-body phase space normalized to the number of events at each energy.

events and is in agreement with the excess events in the $M(\bar{p}\pi^0, p\pi^0)$ mass distribution attributed to $\Delta(1236)$ and $\bar{\Delta}(1236)$ production.

Figure 6 shows the momentum-transfer distributions for the three energies combined. The distributions expected to be the same from charge-conjugation invariance have been combined. The curve labeled PS is the distribution expected from phase space normalized to the number of events at each energy. The experimental distributions, especially those shown in Fig. 6(c), are peaked more toward low momentum transfer.

Soft-Pion Model. Since the energy region studied is very near threshold, it is attractive to compare results with current-algebra predictions of soft-pion emission which relate the inelastic single-pion production to elastic scattering. Although there are some important kinematical ambiguities (connected with treating the soft pion in the real world), this model has the appealing feature that there are intrinsically no free parameters. Analogous calculations of single soft-pion production in pp and pn collisions have been carried out by Beder⁶ and Schillaci *et al.*⁷ and provide a reasonable description for single-pion production in low-energy NN reactions.

Our calculation parallels those of the $NN \rightarrow NN\pi$ reactions. The soft-pion emission amplitude is obtained by application of the canonical procedures, by now well known.⁸ As usual, only emission from external particles is retained in the limit of zero pion four-momentum. For simplicity, the amplitude is evaluated at threshold; in this case the final nucleons cannot emit soft pions and the only contributing diagrams are those of Fig. 7. All possible threshold approximations are made, and only terms of order m/M , where m is the pion mass and M is the nucleon mass, are retained. The result is

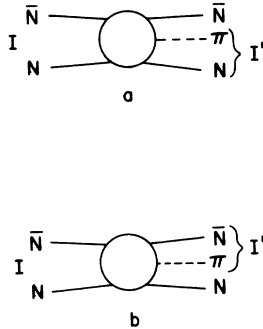


FIG. 5. Generalized diagrams for $\bar{N}N \rightarrow \bar{N}N\pi\pi$ defining isospin variables.

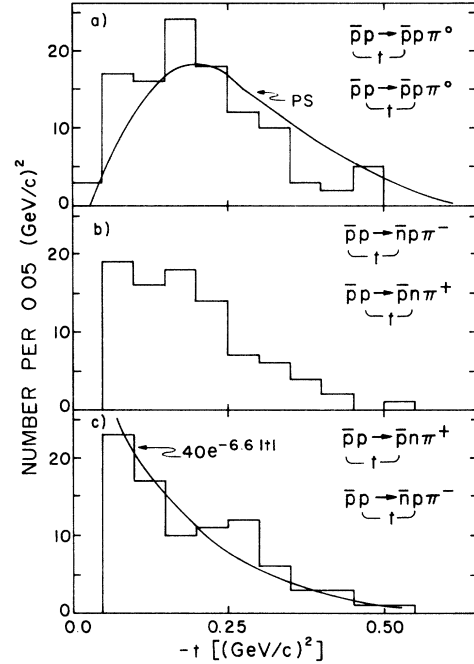


FIG. 6. Momentum-transfer-squared distributions for the $\bar{N}N \rightarrow \bar{N}N\pi$ reactions. Charge-conjugate distributions have been combined. The distributions contain all three energies. The curve labeled PS is calculated according to phase space and is approximately the same for all three distributions. The bottom curve is the result of a fit of this data to the function $Ae^{-b|t|}$.

$$\sigma_{\bar{N}N\pi} = \left(\frac{g^2}{4\pi}\right) \frac{1}{8\sqrt{2}} \left(\frac{\epsilon}{M}\right)^2 \frac{m}{M} \bar{\sigma}_{\bar{N}N},$$

where

$$\bar{\sigma}_{\bar{N}N} = \frac{\int_0^\epsilon d\eta [\eta(\epsilon - \eta)]^{1/2} \sigma_{\bar{N}N}(\eta)}{\int_0^\epsilon d\eta [\eta(\epsilon - \eta)]^{1/2}},$$

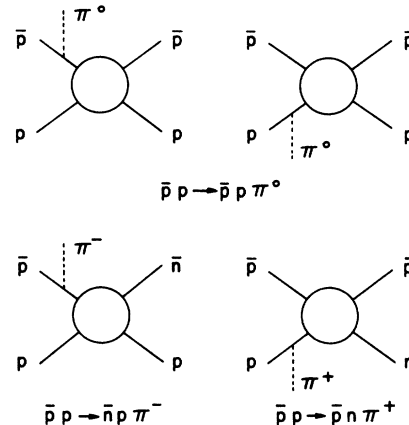


FIG. 7. Soft-pion diagrams contributing to $\bar{N}N \rightarrow \bar{N}N\pi$ in the threshold approximation.

$g^2/4\pi \cong 15$, $\epsilon = W - 2M - m$, W is the total c.m. energy, and $\sigma_{\bar{N}N}(\eta)$ is the nucleon-antinucleon elastic cross section (averaged over angles) which is a function of the total $\bar{N}N$ center-of-mass kinetic energy η . The result is the same for the neutral- and charged-pion production channels essentially because even though only one diagram contributes to the π^\pm case, the charged-pion coupling constant is $\sqrt{2}$ times the neutral-pion coupling constant.

An assumption invoked in obtaining these results is that of spin independence in the $\bar{N}N$ elastic scattering. For example, an explicit calculation in terms of the low-energy S -wave singlet and triplet spin cross sections, σ_s and σ_t , gives the above result with combinations $\frac{1}{2}(\sigma_s + \sigma_t)$ and $\frac{1}{4}(\sigma_s + 3\sigma_t)$ for π^0 and π^\pm , respectively. Spin independence, i.e., the equality of σ_s and σ_t , appears to be a reasonable assumption for $\bar{N}N$ scattering.

The evaluation of $\bar{\sigma}_{\bar{N}N}$ is ambiguous both in the choice of variable parametrizing the elastic scattering cross section and in the model employed for the off-shell correction. It is by no means clear whether the cross section should be evaluated at the energy of the initial or final $\bar{N}N$ systems, or at some point in between. In particular, if the initial \bar{N} and N momenta are defined as p_1 and p_2 and the final momenta as p_3 and p_4 , then the energy of the $\bar{N}N$ system can be defined in terms of $2p_1 \cdot p_2$, $p_1 \cdot p_2 + p_3 \cdot p_4$, or $2p_3 \cdot p_4$, which are all equivalent for elastic scattering. However, for pion emission at incident beam momenta of 1 GeV/c, these give maximum lab kinetic energies at which to evaluate the elastic scattering cross sections of about 430, 290, and 140 MeV, respectively. Since the pion emission is only from the initial nucleon or antinucleon, $p_3 \cdot p_4$ is perhaps the most appropriate choice of variable to evaluate the elastic cross section. We approximate the off-shell cross section by the physical cross section evaluated at the energy given by the final $\bar{N}N$ system.

Furthermore, the present lack of detailed low-energy $\bar{p}p$ and $\bar{p}n$ elastic scattering data makes accurate calculation of $\bar{\sigma}_{\bar{N}N}$ impossible. We estimate⁹ the relevant values of $\bar{\sigma}_{\bar{p}p}$ for our energy region to be approximately constant and 70 mb. We also take $\bar{\sigma}_{\bar{p}n} = \bar{\sigma}_{\bar{p}p}$. For our three energies we calculate $\sigma_{\bar{N}N\pi}$ to be 41, 103, and 161 μb for the neutral-pion channel and 33, 92, and 147 μb for the charged-pion channels. These soft-pion results are shown on Figs. 1 and 2 labeled SP. The calculated cross sections are about a factor of two greater than the data.

Schillaci *et al.*⁷ have parametrized the NN elastic scattering in terms of $p_1 \cdot p_2 + p_3 \cdot p_4$, which in our case would reduce the cross sections by about

25%. They also employ a specific model to account for the off-shell scattering, which gives an additional factor of

$$\frac{32}{15\pi} \left(\frac{\epsilon}{m} \right)^{1/2} \approx \frac{1}{2}.$$

One consequence of (this version of) the calculation is that

$$R \cong (1.1 \text{ to } 1.2) \frac{\sigma_{\bar{p}p}}{\sigma_{\bar{p}n}}.$$

Our data, as noted above in the phase-space fit, tend to favor an average value for $R = 1.0 \pm 0.2$ and are consistent with the prediction based on $\sigma_{\bar{p}n} \approx \sigma_{\bar{p}p}$.

In this soft-pion calculation the pion is isotropic and the nucleon-antinucleon elastic scattering dynamics are taken only in an average sense and are almost constant. Therefore, most of the energy variation of the cross section is due to the increasing phase-space volume, and it is not surprising that the shape is similar to the phase-space calculation. The soft-pion model does provide a definite prediction for the normalization, which gives a reasonable approximation¹⁰ to the data.

The soft-pion model may be used to qualitatively explain the features of the momentum-transfer distributions of Fig. 6. In particular, Fig. 6(c) is the distribution of the momentum transfer between the initial and final proton (and antiproton) which does not emit the charged pion. One expects this distribution to be approximately the same as the elastic momentum-transfer distribution, and indeed, it is sharply peaked at low momentum-transfer values. The curve drawn on this distribution is $40e^{-6.6|t|}$. Even though this slope parameter of 6.6 (GeV/c)⁻² is about an order of magnitude less than the slope parameters determined for low-energy $\bar{N}N$ elastic scattering,⁹ the qualitative feature of steep exponential dependence on $|t|$ is present. Figure 6(b) is the momentum transfer for the proton (or antiproton) which emits the charged pion and does not exhibit the rapid decrease with increasing momentum transfer. Since there is no way to establish which initial particle emits the neutral pion in the $\bar{p}p \rightarrow \bar{p}p\pi^0$ reaction, Fig. 6(a) is the sum of two such distributions. The shape of this distribution is not inconsistent with being a sum of the other [i.e., 6(b) and 6(c)] two distributions.

One-Pion-Exchange Model. We have also tried calculations based on the usual one-pion-exchange model with various vertex corrections. The cross sections and momentum-transfer distributions are poorly fitted by this model.

VI. CONCLUSIONS

Resonance production at our low energies is small, but there is a possible enhancement with $I=1$ favored which may be the $S(1930)$. Our highest-energy $\bar{p}p \rightarrow \bar{p}p\pi^0$ channel may proceed approximately 50% through $\Delta(1236)\bar{p} + \Delta(1236)p$.

The cross section for $\bar{p}p \rightarrow \bar{N}N\pi$ as a function of energy shows no major anomaly in this energy region, i.e., it is relatively well explained by the soft-pion dynamical mechanism and, at the very least, obeys the energy dependence of phase space, joining smoothly onto data at higher energies. This fact may be interpreted as evidence against the quark model proposed by Faiman, Goldhaber, and Zarmi¹¹ which predicts nonstrange exotic mesons (composed of $qq\bar{q}\bar{q}$) at mass ≈ 2.075 GeV/ c^2 , coupled preferentially to $\bar{N}N$ and $\bar{N}N\pi$. The existence of such exotic states coupled primarily to baryon-antibaryon and not to multimeson systems was predicted originally by Rosner¹²; the model of Faiman *et al.* yields degenerate $I=1$ states with $J^P = 2^+, 1^+$, and 0^+ above $\bar{N}N\pi$ threshold as indi-

cated above. Unless the widths were quite small (i.e., of the order of a few MeV or less) detection of formation of these resonant states in the experiment reported here would be expected with sensitivity considerably greater than in either the $\bar{N}N$ elastic or total cross sections. Also, as pointed out by Rosner,¹² observation of such resonances in $\bar{N}N$ or $\bar{N}N\pi$ subsystems produced in $\bar{p}p$ or $\bar{p}d$ reactions may be obscured by strong competition from isobar production. No such difficulty confronts observation in the formation experiment described here. As indicated above, we see no evidence for the predicted exotic states.

ACKNOWLEDGMENTS

We wish to thank the bubble-chamber crews and the AGS operations staff, and our scanning group for their essential contributions. One of us (J.S.) would like to acknowledge a useful discussion with N. Cabibbo and G. Preparata on the subject of the soft-pion mechanism, and D. Faiman for a discussion of the quark-model predictions.

*Work performed under the auspices of the U. S. Atomic Energy Commission.

¹T. C. Bacon, I. Butterworth, R. J. Miller, J. J. Phelan, R. A. Donald, D. N. Edwards, D. C. Howard, and R. S. Moore, Nucl. Phys. **B32**, 66 (1971); P. S. Eastman, Z. Ming Ma, B. Y. Oh, D. L. Parker, G. A. Smith, and R. J. Sprafka, Nucl. Phys. **B51**, 29 (1973); G. R. Lynch, R. E. Foulks, G. R. Kalbfleisch, S. L. Limentani, J. B. Shafer, M. L. Stevenson, and N. Xuong, Phys. Rev. **131**, 1276 (1963); T. A. Stringer, N. Kwak, G. H. Mall, J. E. Manweiler, and R. Stump, Nucl. Phys. **B32**, 486 (1971); R. Sears, R. Socash, and L. Marshall Libby, Phys. Lett. **29B**, 700 (1969); T. Ferbel, A. Firestone, J. Sandweiss, H. D. Taft, M. Gailloud, T. W. Morris, A. H. Bachman, P. Baumel, and R. M. Lea, Phys. Rev. **137**, B1250 (1965); H. C. Dehne, E. Raubold, P. Söding, M. W. Teucher, and G. Wolf, Phys. Lett. **9B**, 185 (1964); H. C. Dehne, E. Lohrmann, E. Raubold, P. Söding, M. W. Teucher, and G. Wolf, Phys. Rev. **136**, B843 (1964); T. Hofmohl, Nukleonika **9**, 121 (1964); O. Czyżewski, B. Escoubes, Y. Goldschmidt-Clermont, M. Guinea-Moorhead, T. Hofmohl, D. R. O. Morrison, and S. de Unamuno-Escoubes, *Proceedings of the Twelfth International Conference on High Energy Physics, Dubna, 1964*, edited by Ya. A. Smorodinskii *et al.* (Atomizdat., Moscow, U.S.S.R., 1966) p. 148; K. Böckmann, B. Nellen, E. Paul, B. Wagini, I. Borecka, J. Diaz, U. Heeren, U. Liebermeister, E. Lohrmann, E. Raubold, P. Söding, S. Wolff, J. Kidd, L. Mandelli, L. Mosca, V. Pelosi, S. Ratti, and L. Tallone, Nuovo Cimento **42A**, 954 (1966); T. Ferbel, J. A. Johnson, H. L. Kraybill, J. Sand-

weiss, and H. D. Taft, Phys. Rev. **173**, 1307 (1968); W. A. Cooper, L. G. Hyman, W. Manner, B. Musgrave, and L. Voyvodic, Phys. Rev. Lett. **20**, 1059 (1968).

²Z. Ming Ma, J. Mountz, P. Zeman, and G. A. Smith, Nucl. Phys. **B68**, 214 (1974).

³M. A. Mandelkern, R. R. Burns, P. E. Condon, and J. Schultz, Phys. Rev. D **8**, 1286 (1973).

⁴D. Cline, J. English, D. D. Reeder, R. Terrell, and J. Twitty, Phys. Rev. Lett. **21**, 1268 (1968).

⁵A. S. Carroll, I-H. Chiang, T. F. Kycia, K. K. Li, P. O. Mazur, D. N. Michael, P. Mockett, D. C. Rahm, and R. Rubinstein, Phys. Rev. Lett. **32**, 247 (1974).

⁶D. S. Beder, Nuovo Cimento **56A**, 625 (1968).

⁷M. E. Schillaci, R. R. Silbar, and J. E. Young, Phys. Rev. Lett. **21**, 711 (1968); Phys. Rev. **179**, 1539 (1969).

⁸J. J. Sakurai, *Currents and Mesons* (University of Chicago Press, Chicago, 1969), Ch. 5.

⁹Particle Data Group, LBL Report No. LBL-58, (unpublished).

¹⁰One may expect that the soft-pion formalism should work best if, during a smooth variation of the pion mass from zero to its true value, other parameters of the system remain roughly constant. Here, the $\bar{N}N$ elastic cross section changes from about 40 mb when the pion is massless (e.g., evaluated at about 430 MeV) to about 70 mb when the pion mass is included in the kinematics as above.

¹¹D. Faiman, G. Goldhaber, and Y. Zarmi, Phys. Lett. **43B**, 307 (1973); D. Faiman, in *Baryon Resonances—73*, Proceedings of the Purdue Conference on Baryon Resonances, 1973, edited by E. C. Fowler (Purdue Univ. Press, Lafayette, Indiana, 1973), p. 233.

¹²J. Rosner, Phys. Rev. Lett. **21**, 950 (1968).